Supporting Information for

Using Quantitative Structural Property Relationships, Chemical Fate Models, and the Chemical Partitioning Space to Investigate the Potential for Long Range Transport and Bioaccumulation of Complex Halogenated Chemical Mixtures

Anya Gawor and Frank Wania*

Department of Physical and Environmental Sciences and Department of Chemistry, University of Toronto Scarborough, 1265 Military Trail, Toronto, Ontario, Canada M1C 1A4

Table S1. Screening criteria for persistent, bioaccumulative, and toxic (PBT) substances used by various regulatory agencies.

Criterion	UNEP [a]	CMP [b]	US EPA [c] (Ban pending)	REACH (PBT) [d]	REACH (vPvB) [d]
Persistence					
$t_{1/2,\ water}$	> 2 months	≥ 182 days	> 180 days	> 60 days (marine) > 40 days (fresh)	> 60 days (marine) > 60 days (fresh)
$t_{1/2,\ soil}$	> 6 months	≥ 182 days	> 180 days	> 120 days	> 180 days
$t_{1/2,\ sediment}$	> 6 months	≥ 365 days	> 180 days	> 180 days (marine) > 120 days (fresh)	> 180 days (marine) > 180 days (fresh)
Bioaccumulation					
BCF/BAF	> 5,000	> 5,000	> 5,000	> 2,000	> 5,000
BMF				> 1	> 1
log K_{OW}	> 5	> 5		> 4.5	> 4.5
Long-range transport					
$t_{1/2,\ air}$	> 2 days	≥ 2 days		N/A	N/A
Toxicity					
	Evidence on toxicity	Inherently toxic	In fish (<0.1mg/L)	NOEC (long-term) < 0.10 mg/L (water organisms); Classified as carcinogenic, mutagenic, toxic for reproduction, other evidence	N/A

[a] Stockholm Convention on POPs. http://www.pops.int/ 2012.[1]

[b] Environment Canada. Guidance Manual for the Risk Evaluation Framework for Sections 199 and 200 of CEPA 1999: Decisions on Environmental Emergency Plans, 2012.[2]

[c] United States Environmental Protection Agency. Category for Persistent, Bioaccumulative, and Toxic New Chemical Substances, 1999.[3]

[d] European Chemicals Agency. Guidance on Information Requirements and Chemical Safety Assessment - Chapter R.11: PBT Assessment. 2012.[4]

Table S2. Version of QSPR software used for chemical property prediction.

Property	**EPISuite™** [a]	**ACD/ADMESuite** [b]	**IFS** [c]
log K_{OW}	KowWin v1.68	logP (AB/LogP v2.0), logP (ACD/Labs), ACD/Absolv	
log K_{AW}	HenryWin v3.2	ACD/Absolv	
log K_{OA}	KoaWin v1.1	ACD/Absolv	
Degradation half-life in air	AOPWin v1.92		
Degradation half-life in fish	BCFBAF v3.01		IFS

[a] United States Environmental Protection Agency. Estimation Programs Interface Suite™ for Microsoft® Windows, v 4.10; 2011.[5]

[b] ACD/ADME Suite 5.0 - Advanced Chemistry Development, Inc v 12.0, Toronto, ON, Canada.[6]

[c] Brown, T. N.; Arnot, J. A.; Wania, F. Iterative fragment selection: A group contribution approach to predicting fish biotransformation half-lives. *Environ. Sci. Technol.* **2012**, *46*, 8253–8260.[7]

Section S1: Comparison of QSPR Predictions with Literature Values for Partitioning Properties and Rationale for QSPR Selection

Table S3 lists the slope, intercept and r^2 of the regressions between measured and predicted partitioning properties, as well as the root mean square error (RMSE).

Most measured data are K_{OW}s. Generally, the K_{OW}s derived from ACD/ADME Suite were judged most similar to the experimental values, based on proximity of data pairs to the 1:1 line (Fig. S1) and the generally good regressions (Table S3).

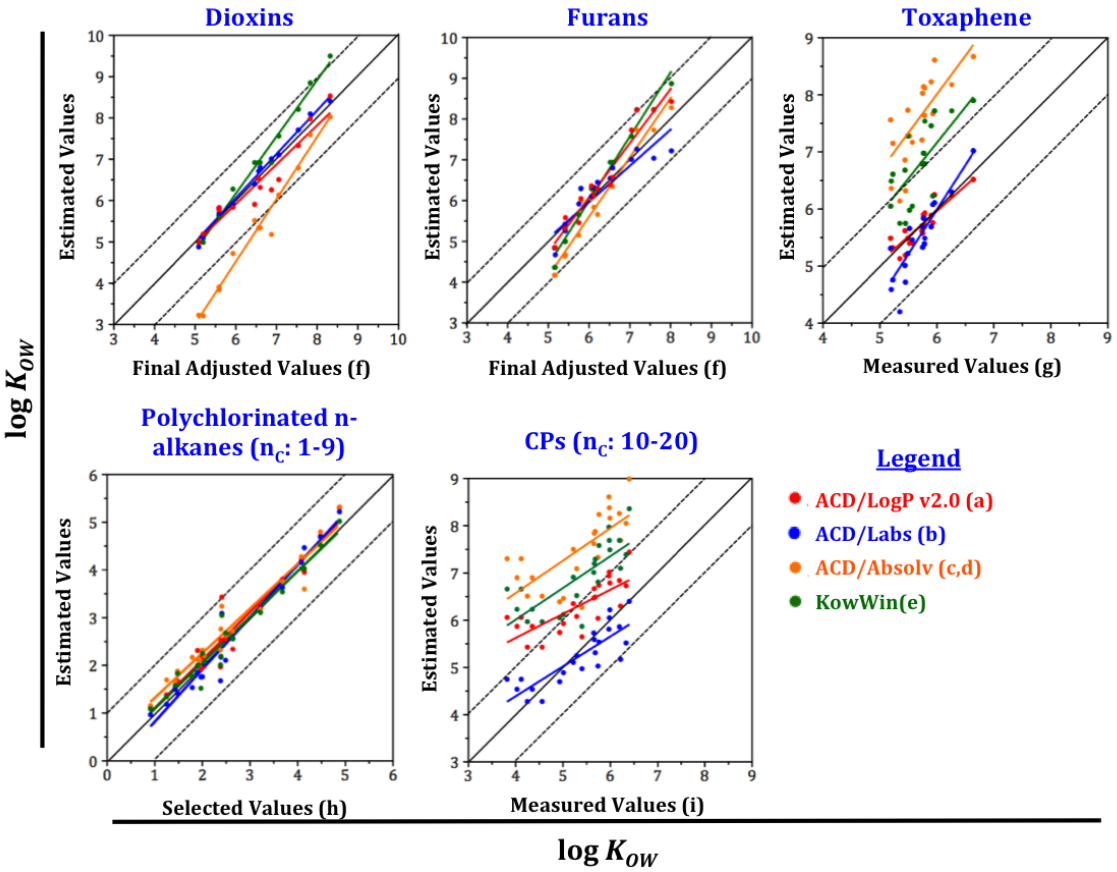

Figure S1. Plots of data comparing values using different estimated techniques (y-axis) vs literature values (x-axis) of log K_{OW}. a) AB/LogP v2.0, b) ACD/Labs, c) ACD/Absolv and d) linear solvation energy relationship by Abraham et al.[8], e) KowWin v1.68, f) Final adjusted values,[9] g) Measured values based on 'slow stir' method[10], h) Selected values based on measured and estimated data[11], i) Measured values averaged from refs.[12,13]

There are very limited (or no) experimental data for the K_{AW} and K_{OA} of the investigated mixtures. Consequently, the selection of a QSPR was based on how well it estimated the properties of constituents of other mixtures with well-established partitioning coefficients. For example, QSPRs for the CPs were selected based on their performance for chlorinated alkanes with less than 9 carbons. Table S3 includes explanations why a certain QSPR was selected for a mixture with no measured values.

Table S3. Results of the comparsion of QSPR predictions with literature values, along with chosen method based on slopes, y-intercepts and goodness-of-fit values.

Log K_{OW}	Slope	Y-Int	R^2	RMSE	Selected
DIBENZO-*P*-DIOXINS					
AB/LogP	0.95	0.21	0.91	0.29	
ACD/Labs	1.10	-0.31	0.99	0.12	√
ACD/Absolv[a]	1.50	-4.5	0.98	0.23	
KowWin	1.40	-2.1	0.99	0.16	
DIBENZOFURANS					
AB/LogP	1.30	-1.9	0.95	0.26	
ACD/Labs	0.89	0.64	0.85	0.31	√
ACD/Absolv[a]	1.50	-3.1	0.96	0.26	
KowWin	1.60	-3.4	0.97	0.25	
TOXAPHENE					
AB/LogP	0.89	0.63	0.84	0.15	√
ACD/Labs	1.60	-3.4	0.83	0.27	
ACD/Absolv[a]	1.40	-0.10	0.58	0.45	
KowWin	1.30	-0.36	0.56	0.43	
POLYCHLORINATED N-ALKANES (n_C:1-9)					
AB/LogP	1.00	0.09	0.94	0.29	√
ACD/Labs	1.10	-0.27	0.96	0.26	
ACD/Absolv[a]	0.94	0.38	0.94	0.25	
KowWin	0.96	0.14	0.95	0.23	
CHLORINATED PARAFFINS (n_C: 10-20)					
AB/LogP	0.51	3.60	0.58	0.34	
ACD/Labs	0.63	1.90	0.70	0.32	√
ACD/Absolv[a]	0.69	3.80	0.50	0.53	
KowWin	0.67	3.30	0.57	0.46	

[a] Calculated using LSER equation 3 from Abraham et al.[14]

Log K_{AW}	Slope	Y-Int	R^2	RMSE	Selected
DIBENZO-*P*-DIOXINS					
ACD/Absolv[b]	-1.50	-8.60	0.92	0.13	
ACD/Absolv[c]	-1.70	-9.00	0.90	0.16	
HenryWin	0.83	-1.50	0.80	0.12	√
DIBENZOFURANS					
ACD/Absolv[b]	-0.05	-0.05	0.01	0.16	
ACD/Absolv[c]	-0.13	-0.13	0.04	0.20	
HenryWin	0.76	0.76	0.70	0.15	√
POLYCHLORINATED N-ALKANES (n_C: 1-9)					
ACD/Absolv[b]	0.76	0.50	0.51		√
ACD/Absolv[c]	0.74	0.54	0.51		
HenryWin	0.19	-0.23	0.06		

TOXAPHENE

Selected: HenryWin

Rationale: Based on the structure being more similar to structures of dioxins/furans (cyclical) than short chloroalkanes (linear).

CHLORINATED PARAFFINS (n_C: 10-20)

Selected: ACD/Absolv[b]

Rationale: These longer chain CPs have same structure as short chloroalkanes. Also, there were 4 SCCPs with reported HLC values. The number of values would not provide reliable results, however, including them with the HLC data for vsPCAs established that the combination of Absolv with Abraham's LSER equations gave better prediction than the other QSPRs.

[b] Calculated using LSER equation from Abraham et al.[13]

[c] Calculated using LSER equation from Goss[16]

Log K_{OA}	Slope	Y-Int	R^2	RMSE	Selected
DIBENZO-*P*-DIOXINS					
log(K_{OW}*/K_{AW})[d]	1.19	-0.38	0.98	0.26	√
ACD/Absolv[e]	0.78	2.00	0.99	0.11	
ACD/Absolv[f]	0.78	1.90	0.99	0.11	
KoaWin*[g]	1.50	-3.05	1.00	0.14	
DIBENZOFURANS					
log(K_{OW}*/K_{AW})[d]	1.07	-0.29	0.94	0.33	√
ACD/Absolv[e]	0.98	-0.18	0.98	0.17	
ACD/Absolv[f]	0.98	-0.19	0.98	0.17	
KoaWin*[g]	1.68	-5.90	0.98	0.30	

TOXAPHENE

Selected: log(K_{OW}*/K_{AW})[d]

Rationale: No measured data for toxaphene K_{OA}'s led to using the triangular relationship (K_{OW}*/K_{AW}) using the selected models for these K's.

VSPCAS (n_C: 1-9)

Selected: log(K_{OW}*/K_{AW})[d]

Rationale: Limited measured data for vsPCAs led to using the triangular relationship (K_{OW}*/K_{AW}) using the selected models for these K's.

CHLORINATED PARAFFINS (n_C: 10-20)

Selected: log(K_{OW}*/K_{AW})[d]

Rationale: No measured data for CPs led to using the triangular relationship (K_{OW}*/K_{AW}) using the selected models for these K's.

[d] log K_{OW}* (selected) – log K_{AW} (selected); K_{OW}* adjusted to dry octanol[15]

[e] Calculated using dry octanol LSER from Abraham et al.[8]

[f] Calculated using dry octanol LSER from Abraham et al.[17]

[g] The K_{OA} from EPISuite™ is calculated using the relationship (K_{OA} = K_{OW}/K_{AW})

K_{AW} predictions were evaluated using the final adjusted values (FAVs) for the PCDD/Fs compiled by Åberg et al.[9] and values for the short chlorinated alkanes recommended by Mackay et al.[11] Whereas the K_{AW}*s* of the PCDD/Fs predicted using the solute descriptors from ACD/Absolv and the LSERs by Goss[16] and Abraham et al.[14] did not agree well with the FAVs by Åberg et al.[9] the combination of ACD/Absolv with Abraham[14]'s LSER equation appears to give K_{AW} values for chlorinated alkanes with a chain length between one and twelve carbons that agree better with recommended values[11] than the EPISuite™ predictions (Fig. S2). While K_{AW} for technical toxaphene has been measured,[18,19] no such data for individual toxaphene constituents exist. Consequently, K_{AW} for substances with no reported data were taken from EPISuite if the substance has a cyclical skeleton (i.e. toxaphene and halogenated dioxins and furans), and from the LSER equations by Abraham et al.[13] if the substance is a CP.

The only information we had for K_{OA} were the values recommended for PCDD/Fs by Åberg et al.[9] While K_{OA} values for PCDFs were well predicted using the thermodynamic triangle and the selected K_{OW}* and K_{AW} predictions, the Absolv-predicted solute descriptors in combination with Abraham et al.'s LSER equations[8,17] was superior for predicting the K_{OA}*s* of the PCDDs (Fig. S2). However, the differences between the methods were not large. Given this limited information and to remain consistent, we estimated K_{OA}*s* for the other mixtures by using the thermodynamic triangle and the pure phase K_{OW}^{*}*s*.

Some words of caution on the reliability of the selected values are appropriate: Given the limited number of experimental values for individual constituents that was used to aid in the selection of QSPRs, it is possible that the selected prediction have considerable error. For example, when comparing the K_{OW}*s* of shorter (n_C: 5-11) and longer CPs (n_C: 11+), Hilger et al.[20] observed nonlinear behavior. Another cautionary note applies to the use of the thermodynamic triangle to determine K_{OA}. Here, we applied an empirical relationship,[15] derived from mostly halogenated aromatic and alicyclic compounds, to convert K_{OW}*s* to K_{OW}**s*; however, the wider applicability of this empirical relationship is not well established.[21] We also only considered the two-dimensional structure, thus disregarding the chirality, which is so prevalent in the toxaphene mixture.

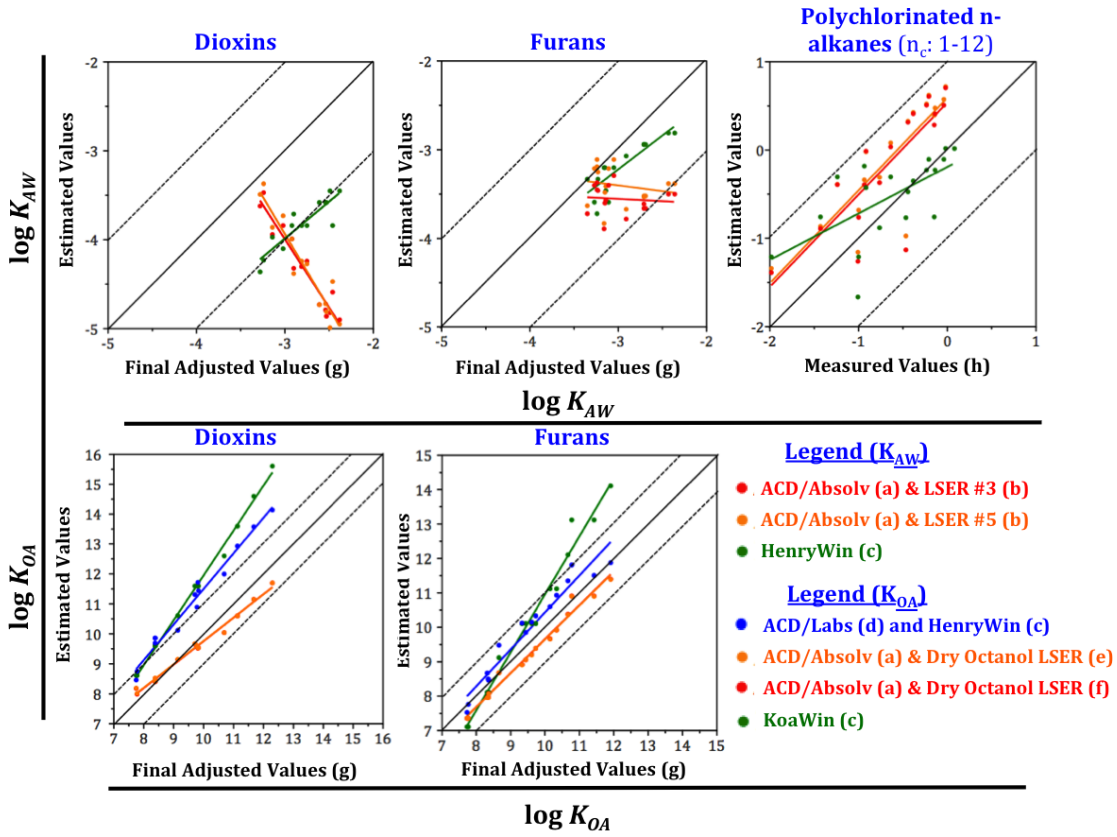

Figure S2. Plots of data comparing values using different estimated techniques (y-axis) vs literature values (x-axis) of log K_{AW} and log K_{OA}. a) ACD/Absolv, b) Linear solvation equation relationship LSER based from Abraham et al.[13] c) KowWin v1.68 and HenryWin v3.2, d) Thermodynamic triangle between adjusted log K_{OW}*'s from ACD/Labs, and log K_{AW}*s* from HenryWin v3.2, e) LSER by Abraham et al.[8] f) LSER by Abraham et al.[17] g) Final Adjusted values from Åberg et al. [9], h) Selected values based on measured and estimated data.[11] Log K_{OA}*s* were calculated considering 'dry' octanol log K_{OW}^{*} derived based on relationships in Beyer et al. [15]

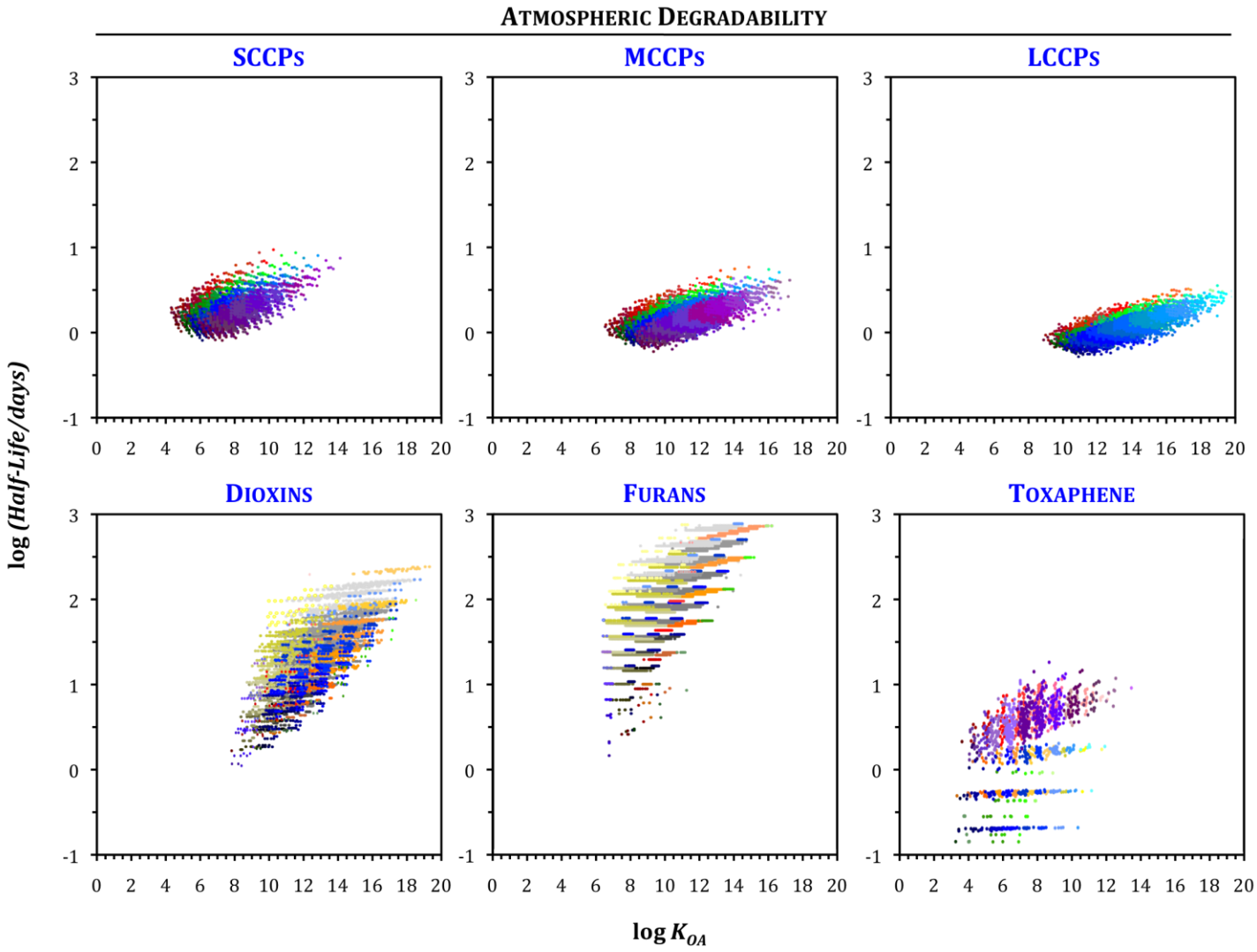

Figure S3: Atmospheric half-lives in days of the mixture components as estimated by AOPWIN. Explanation of the color coding is shown in Fig. 2 in the main paper.

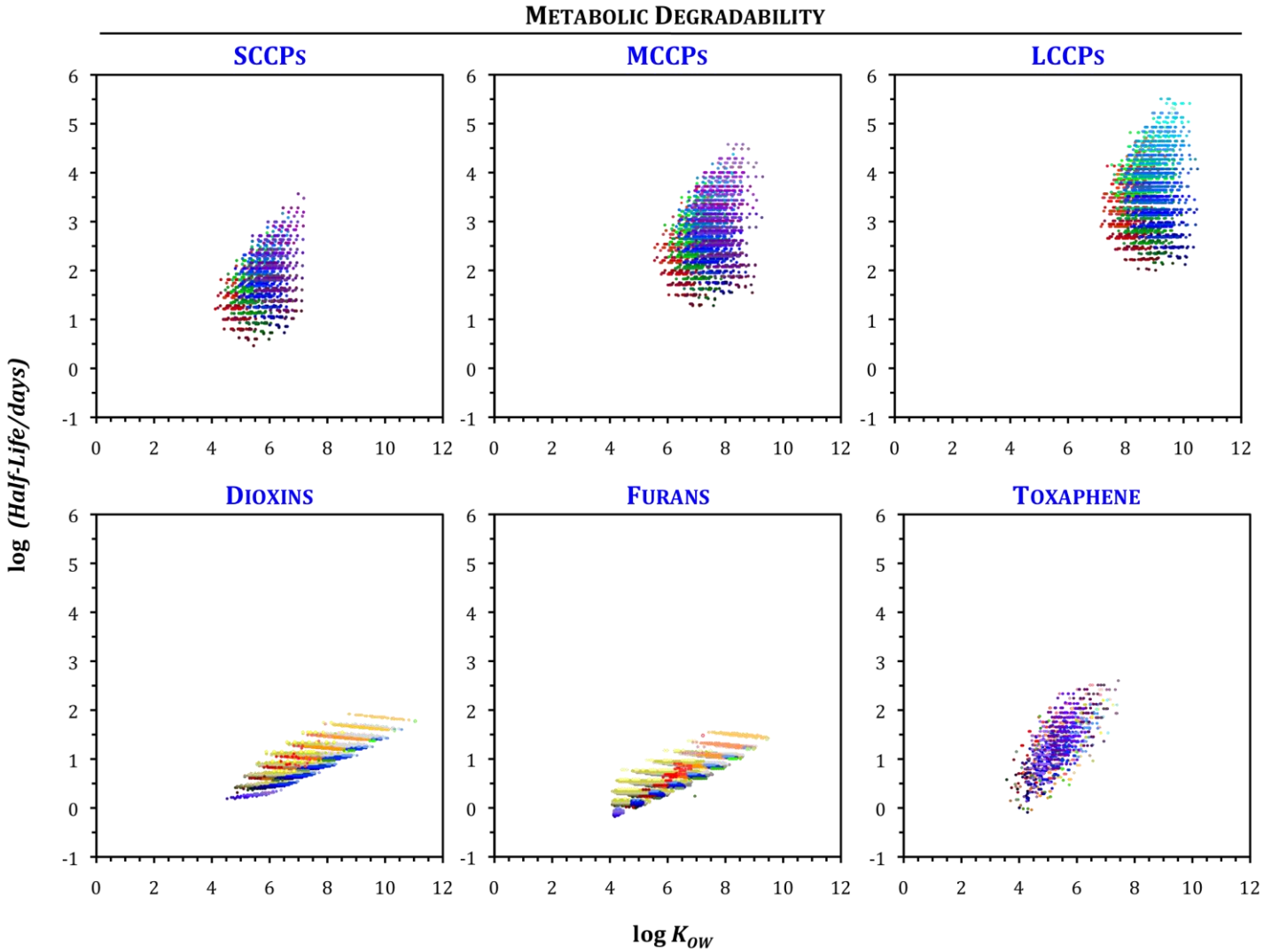

Figure S4: Metabolic degradation half-lives in fish in days of the mixture components as estimated using either: fragment-based QSPR developed through iterative fragment selection (toxaphene), EPISuite™ (dioxins and furans), or average of both (CPs).[7] Explanation of the color coding is shown in Fig. 2 in the main paper.

Table S4. List of chemical space maps utilized in this study.

Name	Description	ref.
Category 1		
Fate in the Overall Environment	Distribution of the chemicals in the overall environment (i.e. air, water, soil/sediment).	22
Environmental Fate in the Atmosphere	Distribution of the chemicals in the atmosphere (i.e. vapour-phase, dissolved in rain drops, sorbed to particles) Dominant deposition processes (i.e. dry gaseous, wet gaseous, wet and dry particle).	23
Environmental Fate in Water	Distribution of the chemicals in water (i.e. dissolved or particle phase).	24
Environmental Fate in Soil	Distribution of chemicals in soil (air pores, water pores, organic solids) and Dominant transport processes (i.e. evaporation, leaching, erosion).	25
Category 2		
Major Mode(s) of Long Range Transport	Assess the major transport pathways of chemicals to undergo long range transport.	26
Arctic Contamination Potential ($eACP_{10}$)	Determines the potential of chemicals to accumulate in the Arctic physical environment based on 10 years of continuous emissions.	27
Environmental Bioaccumulation Potential ($EBAP_{10}$)	Determines the potential of chemicals to bioaccumulate in humans living in the Arctic.	28
Arctic Contamination and Bioaccumulation Potential ($AC\text{-}BAP_{10}$)	Determines the likelihood of chemicals to reach the Arctic AND bioaccumulate in humans living in the Arctic.	28

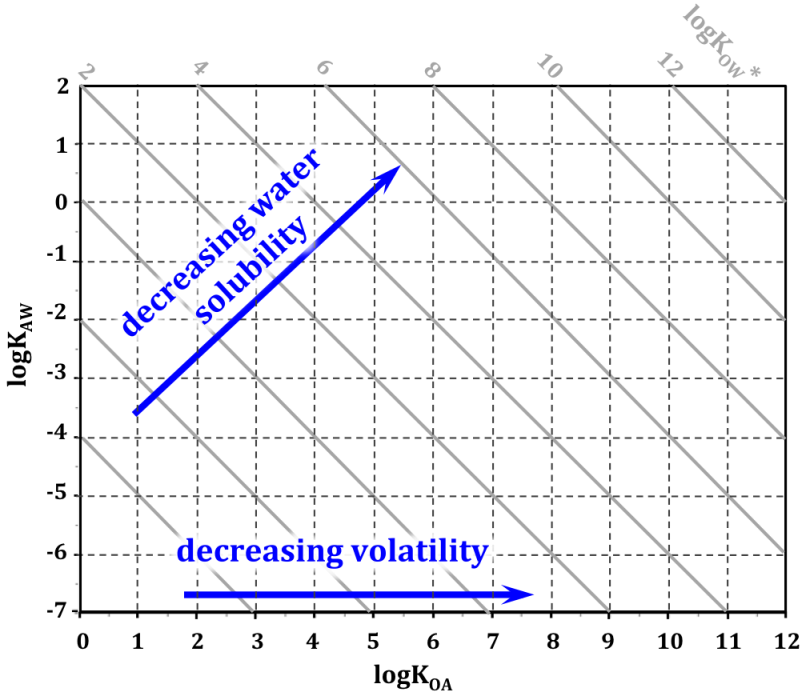

Figure S5. Chemical partitioning space defined by the two partitioning coefficients log K_{OA} and log K_{AW}. Because of the thermodynamic triangle log K_{OW}* = log K_{OA} + log K_{AW}, the grey diagonal lines designate chemicals of equal log K_{OW}*.

Table S5. Partitioning coefficient ranges for the three sets of mixtures.

Chemical Mixture	**log K_{AW}**		**log K_{OA}**	
	Min	*Max*	*Min*	*Max*
Chlorinated Paraffins	- 7.15	1.09	1.61	19.68
SCCPs	- 6.05	1.07	4.07	12.55
MCCPs	-7.66	1.13	5.96	16.09
LCCPs	-8.69	1.00	7.71	18.44
Dioxins and Furans	- 6.52	- 2.14	6.42	17.57
PXDD	- 6.52	- 2.78	7.78	17.57
PXDF	- 5.88	- 2.14	6.42	15.31
PXXDD	- 6.25	- 2.98	8.18	17.07
PXXDF	- 5.61	- 2.34	6.57	15.07
PXXXDD	- 5.78	- 3.45	9.30	16.27
PXXXDF	- 5.14	- 2.81	7.55	14.16
Toxaphene	- 4.56	0.68	3.41	12.34
Bornane	- 4.11	- 0.03	3.77	11.27
Bornene	- 3.55	0.22	3.48	10.81
Bornadiene	-2.07	0.17	3.41	8.32
Camphene	-3.55	0.68	3.58	10.94
Dihydrocamphene	-4.56	- 0.03	4.20	12.34

Section S2: Equilibrium Phase Distribution in Air, Water, Soil and the Whole Environment

Individual constituents of mixtures could vary noticeably in partitioning properties due to structural characteristics (Table S5, Fig. 2). Here, we assessed the equilibrium phase distribution behavior of the chemical mixture constituents and some of the basic environmental fate characteristics that derive from it. We relied on a number of chemical partitioning space maps (Figs. S6 to 10) that have been discussed in detail in other publications. They display a chemical's equilibrium phase distribution in the environment as a whole, [22] in the atmosphere, [23] in water bodies [24] and in the soil environment. [25] The phase distribution in air and soil also impacts the dominant transport mechanisms, which can be displayed in additional sets of chemical partitioning space plots.[23,25]

If a chemical's position falls into one of the areas within the partitioning spaces shaded in a darker red, blue, or green, it is likely to be found predominantly (i.e. >90%) in the gas, aqueous, or organic phase of an environmental compartment. A chemical's position within an area shaded lightly suggests a transitional behavior, with considerable fractions (10-90%) present in more than one phase. The areas of the phases in the different partitioning space maps differ in size from one another as they rely on the relative volumes of the three compartments. An area expands if the phase's volume increases. For example, if the water content in soil increases, the boundary for the blue region in Figs. S8d-f, S9d-f, or S10e shifts upward. The boundaries of the green region in Figs. S6d-f, S7d-f, or S10B shift to the left, when concentration of organic particles in the atmosphere increases.

We only estimated the partitioning coefficients of mixture constituents at 25 °C, even though equilibrium phase distribution of the components is dependent on temperature. Generally, chemicals will move to the lower right in the partitioning spaces with decreasing temperatures, i.e. shift away from the gas phase to the condensed phases. The coloring and shading of the constituents follow the same scheme as in Figure 2.

Equilibrium Phase Distribution in the Environment as a Whole

The first partitioning space map defines the equilibrium phase distribution of a chemical in the environment as a whole (Figs. S6a-c, S7a-c, S9a), i.e., establishes whether a mixture constituent is more likely to be found in the atmosphere, in lakes and rivers, or in soil and sediments of an evaluative environment.[22] While few chemicals indeed reach an equilibrium distribution in the environment as a whole, such basic information can assist in reducing the amount of work invested to collect data of marginal value.[22] For example, while chemicals partitioning predominantly into the air are not likely to elicit POP-like concern, they may be greenhouse gases or

ozone depleting substances. All the parameters used to construct this space plot remained the same as in ref. [22], aside from changing the x-axis from log K_{OW} to log K_{OA} to achieve consistency with the other maps.

Relatively high K_{OA}s and low to moderate K_{AW}s for most mixture constituents means that they can be expected to associate primarily with organic matter in soils and sediments, although the most volatile mixture constituents, particularly a very small number of SCCPs (n_C: 10, n_{Cl}: ~1 – 4; n_C: 11-12, n_{Cl}: 1) and toxaphene constituents with less than four chlorines, may be partitioning predominantly into the atmosphere. Reflecting a high hydrophobicity, none of the constituents of any of the mixtures partitions predominantly into water (Figs. S6a-c, S7a-c, S9a).

LCCPs are strongly associated with organic matter (>90%). The predicted distribution behavior of CPs with n_c above 10 in the environment as a whole, Fig. S6c, is supported by the few studies conducted on these compounds, as reviewed by Feo et al.[29]

Technical toxaphene (TT), which mostly comprises constituents with 6 to 10 chlorines, will mostly be present in soils and sediments, until it undergoes 'weathering'. The less chlorinated forms (n_{Cl}: 1-5) appear to be more dominant in air (Fig. S10a).

Equilibrium Phase Distribution and Depositional Processes in the Atmosphere

The second sets of maps describe the equilibrium distribution between vapor phase, water droplets, and particles in a cloud (Figs. S6d-f, S7d-f) and the resultant atmospheric deposition mechanisms (Figs. S6g-i, S7g-i). They were adapted from Lei and Wania [23] by altering the x- (log $K_{particle/air}$ → log K_{OA}) and y- axes (log $K_{rain/air}$ → log K_{AW}) and adopting a volume fraction of organic aerosol in the atmosphere, v_{OA}, of $1x10^{-11}$, which is half of the volume fraction previously [23] used for particles (v_{PA} = $2x10^{-11}$). Partitioning between organic particles and air is assumed to be the same as partitioning between octanol and air.

The majority of the components of SCCPs (Fig. S6d) and toxaphene (Fig. S10b), will be mostly in the atmospheric vapor phase and undergo dry gaseous deposition. Some highly chlorinated SCCPs and toxaphene components with more than 8 chlorines may start to become particle bound and thus be subject to wet and dry particle deposition (Figs. S6g, S10c). For MCCPs (Figs. S6e and h) and halogenated dioxins and furans (Figs. S7d-i), this transitional phase occurs at moderate halogenation, n_X: 9–10, 2–3, and 4–5, respectively. Due to high K_{OA}s for LCCPs, they will be mostly sorbed to particles (Fig. S6f) and undergo primarily (>50%) particle deposition, starting at ~ 7 chlorines (Fig. S6i). All mixture constituents are relatively hydrophobic, and only a very small fraction (<10%) could possibly be dissolved in

raindrops. Nevertheless, wet vapour scavenging may be a relevant deposition process for some dioxins and furans (Fig. S7g-i) and some SCCPs and MCCPs (Fig. S6g-h), especially at temperatures below 25 °C.

Equilibrium Phase Distribution in Water

Another set of maps (Figs. S8a-c, S9a-c, Fig. S10d) describes the equilibrium phase distribution between dissolved and suspended particle phase in the water column as a function of the chemical's log K_{OW} and the concentration of suspended particles.[24] Despite the result from Figs. S6a-c, S7a-c, and S10a, which suggested that the generally low solubility for the mixture constituents would prevent them from being present in large proportions in water bodies, a variety of studies has reported the presence of these mixtures in water. This can be due to direct emissions (e.g. spills, effluents) or environmental pathways (e.g. run-off, atmospheric deposition). CPs in particular, may be emitted into water.[29,30] Figs. S8a-c, S9a-c, and Fig. S10d were adapted from Meyer et al's [24] by directly using log K_{OW} as the x-axis instead of the log K_{OC} and by extending the range of the y-axis to lower particle concentrations as they may occur in marine waters. The constituents are grouped into rows based on their skeletal structure, number of halogens, or halogen type, following the same color scheme as in Figure 2. The constituents can be located anywhere along the y-axis as the amount of particulate matter in water (log C_{PM} in $mg \cdot L^{-1}$) is not a chemical parameter. It is meant to allow for better visibility and comparability between the different groups within a chemical mixture. The yellow vertical lines indicate the range in log K_{OW}*s* for that mixture. They aid in understanding the distribution of the entire mixture in water at various particle concentrations.

The concentration of particles in water affects the phase distribution of the constituents. In ocean waters, where there is relatively low suspended particle matter compared to other water bodies (less than 1 $mg \cdot L^{-1}$), only components with log K_{OW} > 8.5 would associate with suspended particles. Specifically, LCCPs will be completely particle-bound (Fig. S8c). For shorter CPs, the association with the dissolved or suspended phases depends on the degree of chlorination and the position of the chlorine atoms on the carbon structure. The transition between the two phases for MCCPs will start for components with moderate degrees of chlorination (n_{Cl}: ~4) (Fig. S8b). For halogenated dioxins and furans, those components with ~3 halogens or less will be in the dissolved phase of ocean water, whereby components with 7–8 halogens will be bound completely to suspended solids (Fig. S9a-c). The transition would occur at ~4–5 halogens for dioxins and ~5–6 halogens for furans. Toxaphene in ocean water will be dominantly in the dissolved form (Fig. S10d).

Equilibrium Phase Distribution and Transport Processes in Soils

Finally, the equilibrium distribution of the chemicals among pore water, pore air and organic solids in soils is shown in Figs. S8d-f, S9d-f, and S10e, as are the chemicals' resultant transport characteristics in soil[25] in Figs. S8g-i, S9g-i, and S10f. These equilibrium phase distribution and mobility plots for a typical temperate soil were adapted from Wong and Wania[25] by changing the x- (log K_{OC} → log K_{OA}; scale) and y- axes (scale). The soil used in the creation of the plots had 5% organic carbon, a 25% field capacity water content, and a depth of 0.18 m.

In soil, almost all of the constituents for the three mixtures are expected to sorb completely to organic solids (Figs. S8d-f, S9d-f, S10e). Two transport processes affect the mobility of the mixture constituents in soil: evaporation or particle erosion. Generally, the constituents with less number of halogens or smaller carbon structures would evaporate from soils, while others would only undergo particle erosion (Figs. S8g-i, S9g-i, and S10f). As the mixture components are relatively hydrophobic, most are unlikely to be subject to leaching and reach groundwater, although some SCCPs may be sufficiently water soluble (Fig. S8g). LCCPs' K_{OA}s are high enough for evaporation to be an unlikely fate process (Fig. S8i). According to the Figs. S8g and S8h, SCCPs and MCCPs with 3–4 and 3–5 chlorines respectively, will be subjected to both evaporation and erosion in soils. Any component of these three groups holding less or more chlorines than the aforementioned is subject more to evaporation or erosion in soils. Halogenated dioxins and furans are primarily affected by erosion, aside from PFDFs, and some PCFDFs and PBFDFs (n_X: 1-3), which are equally affected by the three mobility mechanisms (i.e. evaporation, leaching, erosion) (Figs. S9g-i). Toxaphene constituents will either primarily evaporate from soils (n_{Cl}: 1–5) or undergo erosion (n_{Cl}: 7–12), although components dominant in technical toxaphene (n_{Cl}: 6–10) can be affected by either of these two mechanisms (Fig. S10e).

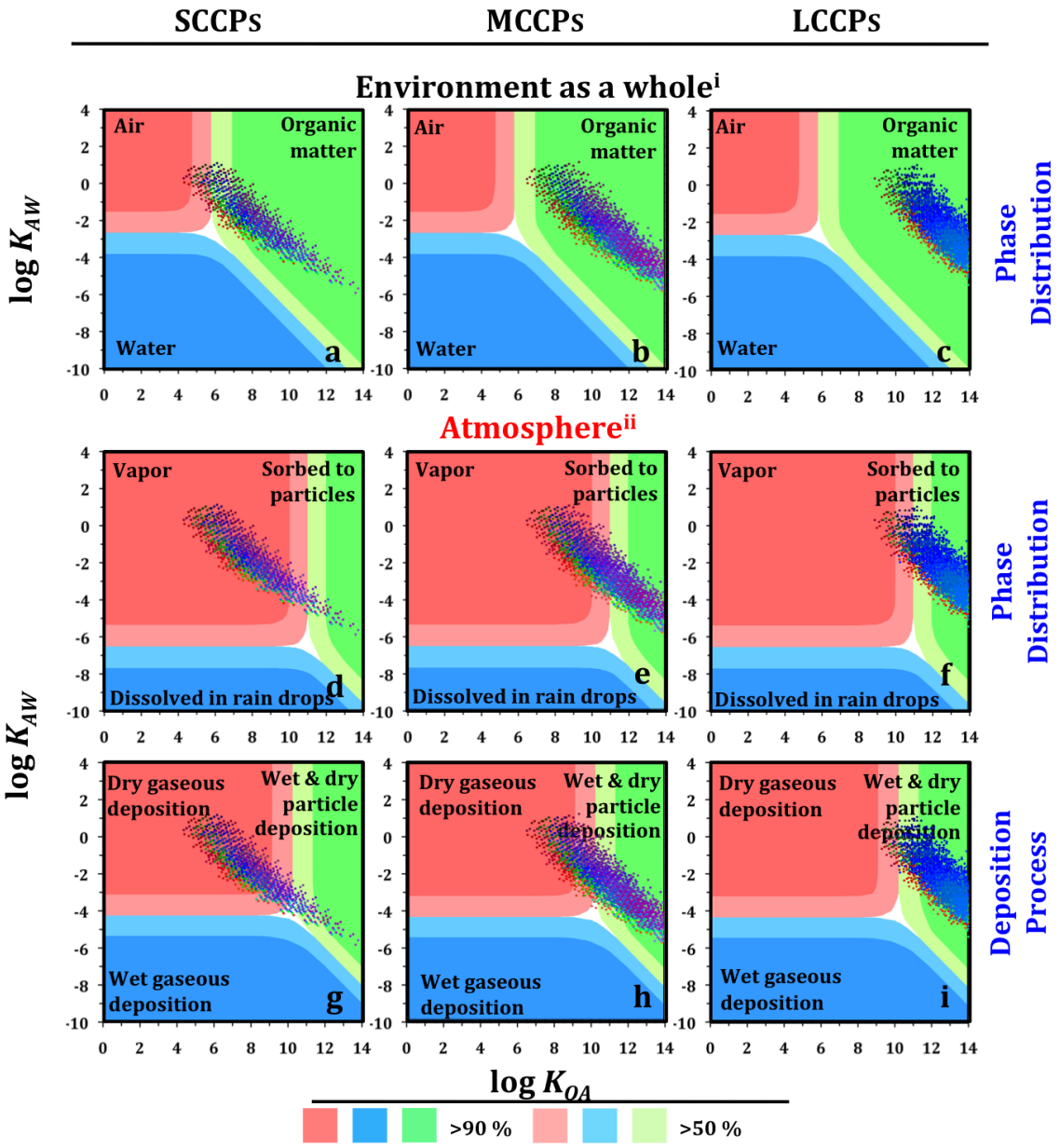

Figure S6. Phase distribution of chlorinated paraffins in the environment as a whole (i),[22] and in a cloud (ii),[23] as well as the dominant atmospheric deposition processes.[23] Color coding for the components displayed as dots within the clouds is shown in Fig. 2 in the main paper.

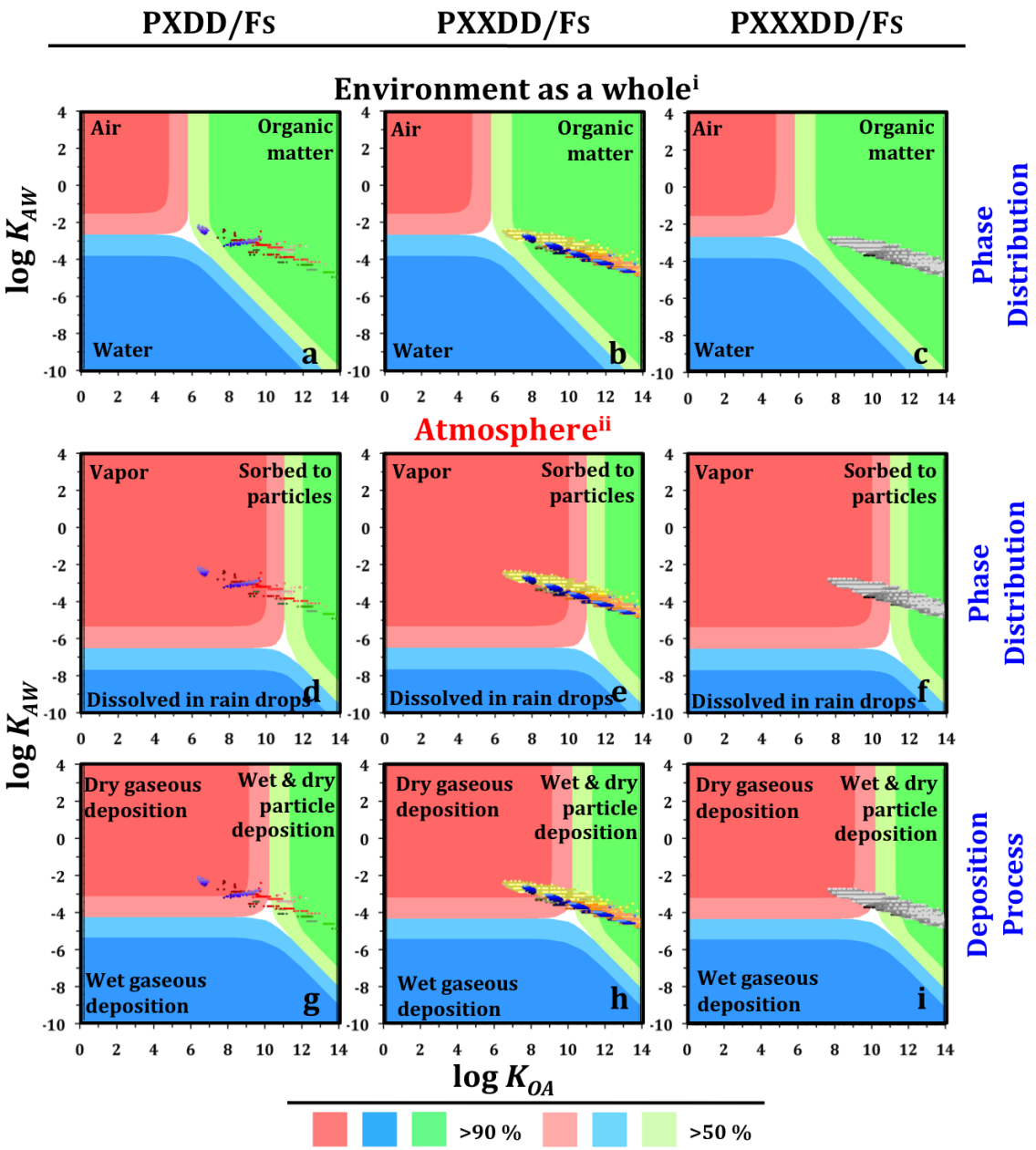

Figure S7. Phase distribution of halogenated dioxins and furans in the environment as a whole (i),[22] and in a cloud (ii),[23] as well as the dominant atmospheric deposition processes.[23] Color coding for the components displayed as dots within the clouds is shown in Fig. 2 in the main paper.

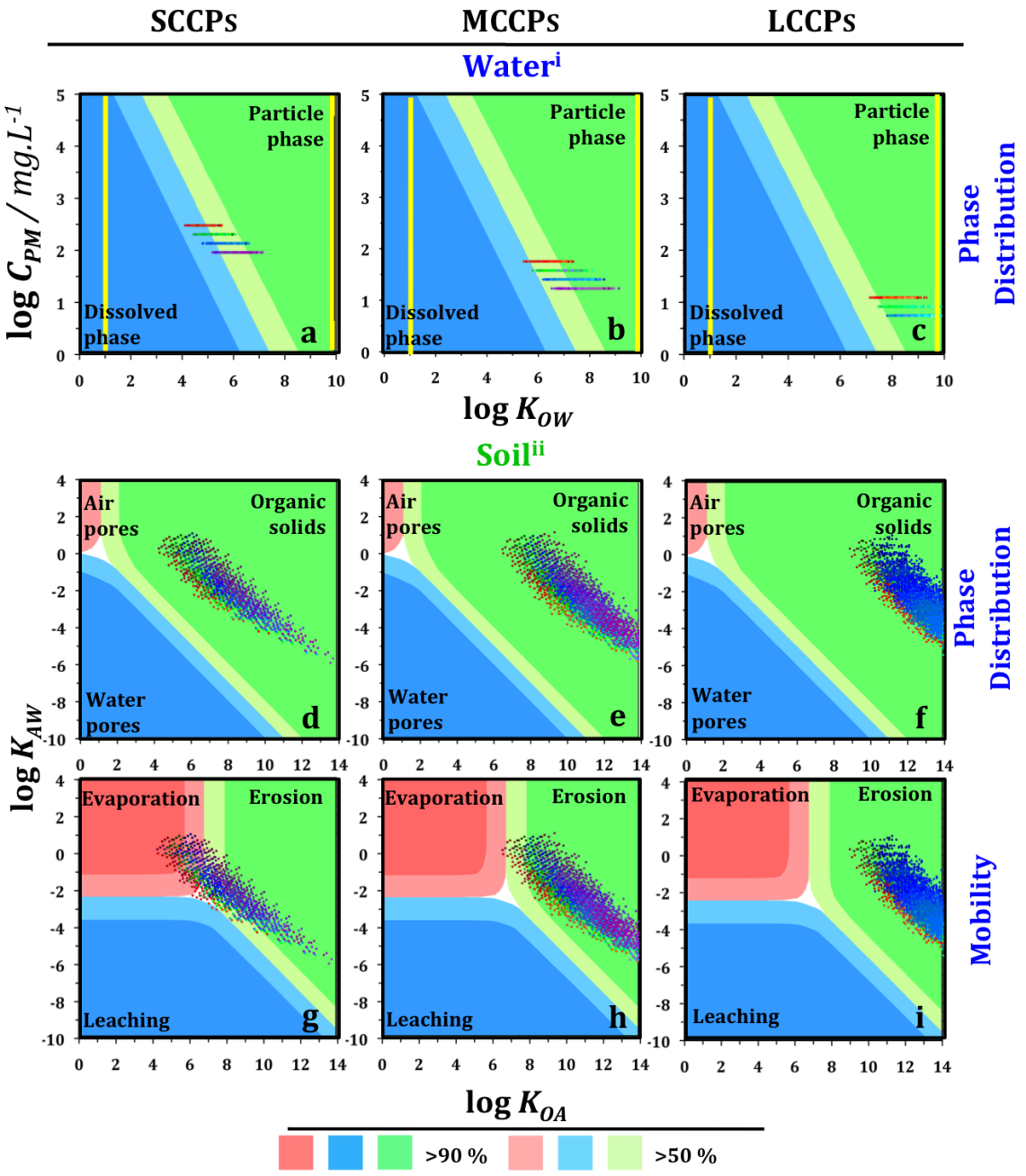

Figure S8. Phase distribution of chlorinated paraffins in water (i)[24] and in soil (ii),[25] and their mobility within soil.[25] The water partitioning plots, a-c, differ from the others in that they display log C_{PM} (concentration of particulate matter, mg·L-1) vs. log K_{OW}. As C_{PM} is an environmental and not a chemical parameter, the constituents can fall anywhere along the y-axis. The yellow lines display the ranges of the log K_{OW} values for the entire mixture. Color coding for the components displayed as dots within the clouds is shown in Fig. 2 in the main paper.

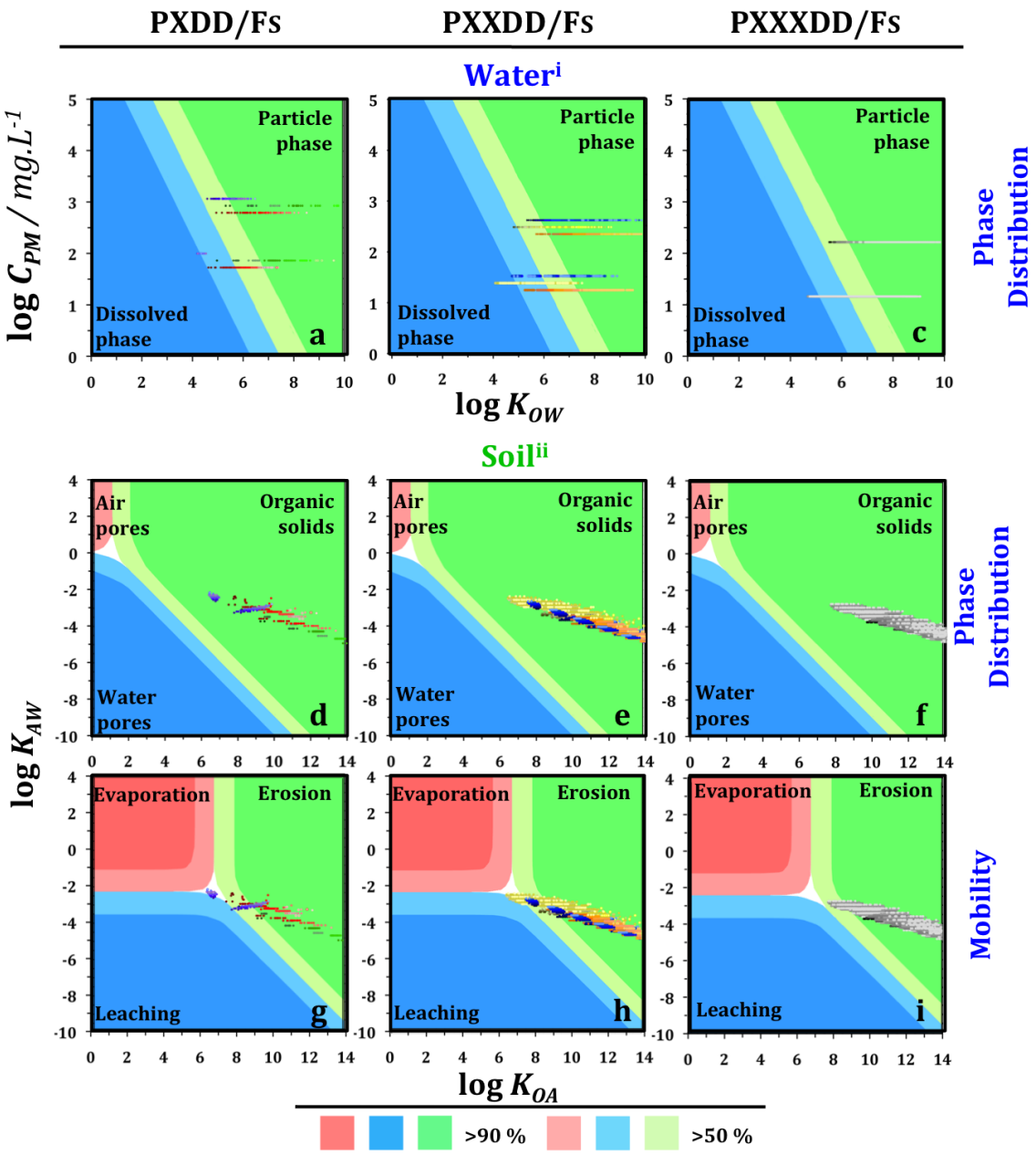

Figure S9. Phase distribution of halogenated dioxins and furans in water (i)[24] and in soil (ii),[25] and their mobility within soil.[25] The water partitioning plots, a-c, differ from the others in that they display log C_{PM} (concentration of particulate matter, mg·L^{-1}) vs. log K_{OW}. . As C_{PM} is an environmental and not a chemical parameter, the constituents can fall anywhere along the y-axis. The yellow lines display the ranges of the log K_{OW} values for the entire mixture. Color coding for the components displayed as dots within the clouds is shown in Fig. 2 in the main paper.

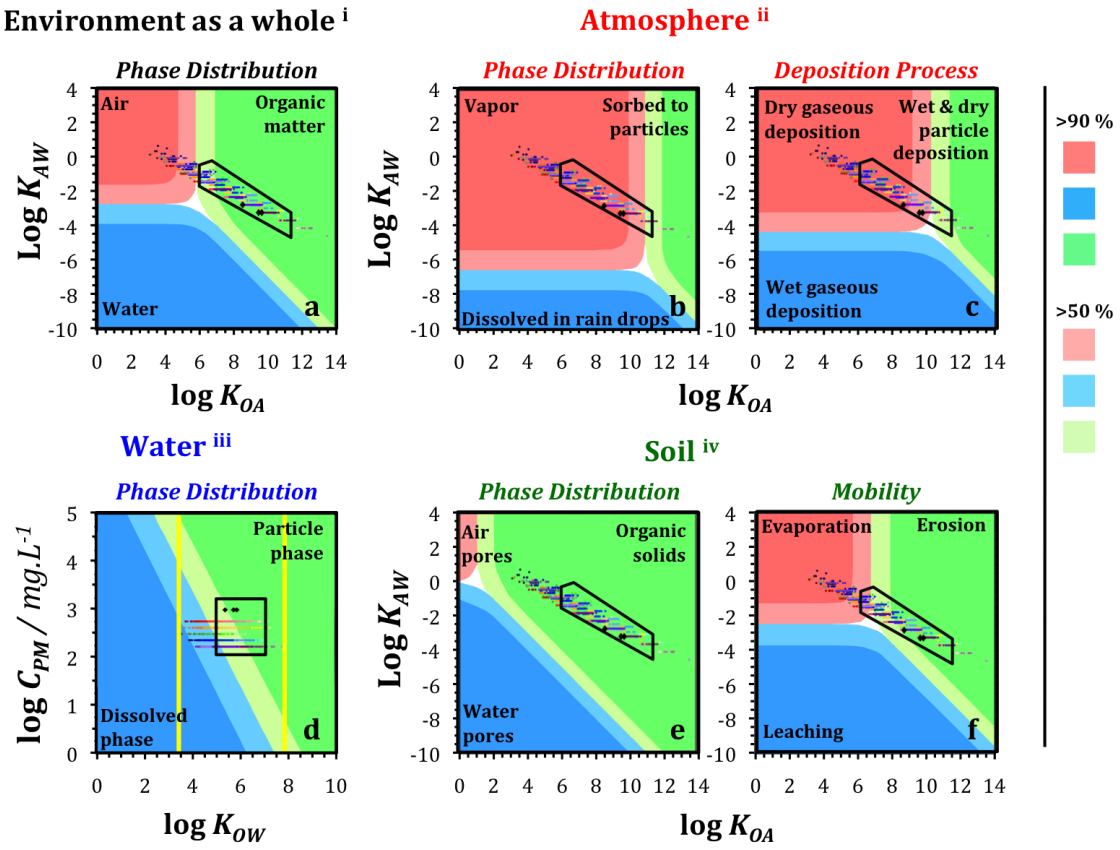

Figure S10. Equilibrium phase distribution of toxaphene components in the environment as a whole (i)[22] in a cloud (ii),[23] in water (iii),[24] and in soil (iv).[25] Also shown are dominant atmospheric deposition processes [23] and the mobility of chemicals within soil.[25] Color coding for the components displayed as dots within the clouds is shown in Fig. 2 in the main paper.

1. UNEP, Interim Secretariat for the Stockholm Convention, United Nations Environmental Programme (UNEP) Chemicals, Geneva, 2001, http://www.pops.int.
2. Environment Canada, *Environment Canada*, 2012, http://www.ec.gc.ca/lcpe-cepa/default.asp?lang=En&n=F1BDDFD0-1&offset=3.
3. US EPA, *Federal Register*, 1999, http://www.epa.gov/fedrgstr/EPA-TOX/1999/November/Day-04/t28888.htm.
4. ECHA, *Regulations,* 2008, **Ch R.11,** *echa.europa.eu.*
5. US EPA, *Estimation Programs Interface Suite™ for Microsoft® Windows, v 4.10*, United States Environmental Protection Agency, Washington, DC, USA.
6. ACD/ADME Suite 5.0, version 12.0, *Advanced Chemistry Development, Inc*, Toronto, ON, Canada, www.acdlabs.com.
7. T. N. Brown, J. A. Arnot, and F. Wania, *Environ. Sci. Technol.*, 2012, **46**, 8253–8260.
8. M. H. Abraham and W. E. Acree Jr, *J Phys Org Chem*, 2008, **21**, 823–832.
9. A. Åberg, M. MacLeod, and K. Wiberg, *J Phys Chem Ref Data*, 2008, **37**, 1997–2008.
10. A. T. Fisk, B. Rosenberg, C. D. Cymbalisty, G. A. Stern, and D. C. G. Muir, *Chemosphere*, 1999, **39**, 2549–2562.
11. D. Mackay, W. Y. Shiu, K.-C. Ma, and S. C. Lee, in *Handbook of Physical-Chemical Properties and Environmental Fate for Organic Chemicals*, Taylor & Francis Group, Boca Raton, FL, 2nd edn. 2006, pp. 921–2257.
12. D. T. H. M. Sijm and T. L. Sinnige, *Chemosphere*, 1995, **31**, 4427–4435.
13. M. H. Abraham, J. Andonian-Haftvan, G. S. Whiting, A. J. Leo, and R. S. Taft, *J. Chem. Soc., Perkin Trans. 2*, 1994, 1777–1791.
14. M. H. Abraham, H. S. Chadha, J. P. Dixon, and A. J. Leo, *J Phys Org Chem*, 1994, **7**, 712–716.
15. A. Beyer, F. Wania, T. Gouin, D. Mackay, and M. Matthies, *Environ. Toxicol. Chem.*, 2002, **21**, 941–953.
16. K.-U. Goss, *Fluid Phase Equilibria*, 2005, **233**, 19–22.
17. M. H. Abraham, J. Le, W. E. Acree, P. W. Carr, and A. J. Dallas, *Chemosphere*, 2001, **44**, 855–863.
18. T. J. Murphy, M. D. Mullin, and J. A. Meyer, *Environ. Sci. Technol.*, 1987, **21**, 155–162.
19. L. M. M. Jantunen and T. F. Bidleman, *Chemosphere - Global Change Science*, 2000, **2**, 225–231.
20. B. Hilger, H. Fromme, W. Völkel, and M. Coelhan, *Environ. Sci. Technol.*, 2011, **45**, 2842–2849.
21. U. Schenker, M. MacLeod, M. Scheringer, and K. Hungerbühler, *Environ. Sci. Technol.*, 2005, **39**, 8434–8441.
22. T. Gouin, D. Mackay, E. Webster, and F. Wania, *Environ. Sci. Technol.*, 2000, **34**, 881–884.
23. Y. D. Lei and F. Wania, *Atmos. Environ.*, 2004, **38**, 3557–3571.
24. T. Meyer, Y. D. Lei, and F. Wania, *Water Research*, 2011, **45**, 1147–1156.

25. F. Wong and F. Wania, *J. Environ. Monit.*, 2011, **13**, 1569–1578.
26. F. Wania, *Environ. Sci. Technol.*, 2006, **40**, 569–577.
27. F. Wania, *Environ. Sci. Technol.*, 2003, **37**, 1344–1351.
28. G. Czub, F. Wania, and M. S. McLachlan, *Environ. Sci. Technol.*, 2008, **42**, 3704–3709.
29. M. L. Feo, E. Eljarrat, D. Barceló, and D. Barceló, *Trends in Analytical Chemistry*, 2009, **28**, 778–791.
30. D. C. G. Muir, in *The Handbook of Environmental Chemistry*, ed. J. Boer, Springer, Berlin, Heidelberg, 2010, vol. 10, pp. 107–133.